Vilnius University
Faculty of Physics
Institute of Applied Electrodynamics and Telecommunications

Vakada Venkata Sai Mohan Revanth

LOW FREQUENCY NOISE CHARACTERISTICS OF COMPOSITES WITH CARBON NANOPARTICLES

Master's Thesis
Electronics and Telecommunications Study Program

Student	Vakada Venkata Sai Mohan Revanth
Approved	2026-05-22
Academic Supervisor	dr. Sandra Pralgauskaitė
Reviewer	dr. Edvardas Kazakevičius
Director of the Institute	dr. Robertas Grigalaitis

Vilnius 2026

Table of Contents

Introduction

In modern electronics, it's very important to know how materials act. We observe the materials that can improve the performance of devices. Things like CNTs are used to make the materials [1].

This study examines the polymer composite materials that integrate multi-walled CNTs (MWCNTs) and metal based conductive fillers. Carbon nanotubes are very good at conducting electricity and are very strong. Carbonized nickel can make charge transport and structural ability better in a composite matrix. By combining these two materials, it is possible to make composites with better and more adjustable electrical properties [1].

This study seeks to examine the resistivity and low-frequency noise attributes of these composite samples under varying conditions and compositions. By looking into how these materials act when different voltages are applied, we will learn more about how they conduct electricity and make noise. These results will help with the larger goal of making advanced electronic materials that work in predictable and controllable way, which is necessary for the next generation of nanoscale electronic systems [1].

The goal of this work is to investigate the resistivity and low-frequency noise characteristics of epoxy composites with MWCNT and Cu@C fillers.

This work is continuous: Vakada Venkata Sai Mohan Revanth, "Resistivity and Low Frequency Noise Characteristics of Composites with Carbon and Nickel Nanoparticles", Electronics and Telecommunications study program master's scientific research work (2025).

1. Literature Review

The first section of the literature review will focus on the material: carbon nanotube composites.

1.1. Carbon Nanotubes

Carbon nanotubes are very good at conducting electricity. Are very strong. Nickel particles can help make these materials more stable. By combining them we can make materials that work better for things like sensors and energy-efficient circuits, and they widely describe the electrical, thermal and mechanical properties in various applications and they have higher aspect ratio. Based on their structural features CNTs are into two types SWCNTs (single-walled carbon nanotubes) and MWCNTs (multi-walled carbon nanotubes) [2].

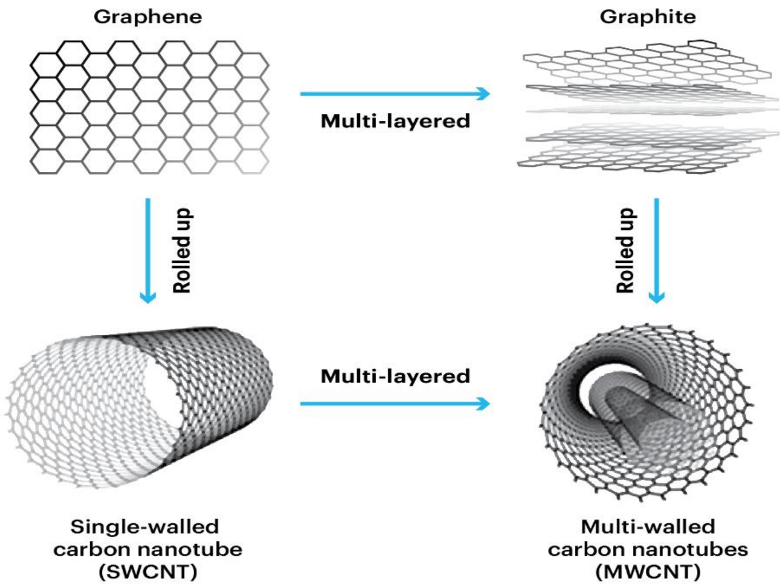

Figure 1.1.1: Structure of SWCNTs and MWCNTs [3].

Notable properties of CNTs include:

- Carbon nanotubes have some interesting mechanical properties that make them useful for strengthening other materials. The strong sp^2 bonds give them high specific strength and tensile strength, which comes from that network. Since they are one-dimensional, they act like fibers [4].
- Electrical Properties. CNTs can be metallic or semiconducting based on their chirality, and they exhibit high electrical conductivity with some SWCNTs having conductivities comparable with cu (copper). The electrical conductivity of CNTs is extremely high, like

graphene and there is a reduction in conductivity of ten growing from SWCNT to MWCNT, this is due to the inter-wall interactions, electron scattering and misalignment of electronic properties of different nanotube layers nestled with one another [4].

- Thermal Properties. CNTs have exceptional thermal conductivity, which means they are efficiently high at transferring heat, and they had such high thermal conductivity because it's due to the graphene structure in which the CNTs are made up of graphene which is a single layer of carbon atoms arranged in a hexagonal lattice. [4].

Carbon Nanotubes are fabricated using various techniques, mainly categorized into top-down and bottom-up (synthesis) methods. The most common bottom-up methods for CNT fabrication include and each synthesis process develops CNTs with different mechanical, electrical and thermal characteristics [5].

Among the many ways CNTs can be fabricated, the primary techniques are arc discharge, chemical vapor deposition (CVD), laser ablation:

Arc discharge. A high-current arc is applied between carbon electrodes in an inert atmosphere, causing carbon to vaporize from CNTs and it happens between two electrodes as arc discharge, the chamber anode is filled with a carbon precursor and the cathode is a pure graphite rod during the process, a constant current is maintained to produce high quality CNTs at high temperature (4000-6000 K). The arc discharge process is reliant on variables such as plasma power, arc current, catalyst, electrode geometry and the catalyst effect in synthesis shown in the size of CNTs can be affected by using the proper size of metal catalyst particles that play an important role in the yield of CNTs. The metal particles encapsulate carbon vapors to form SWCNTs [5].

Chemical vapor deposition (CVD*)*. Hydrocarbon gases like (e.g. methane) decompose on a metal catalyst at high temperatures providing CNT growth and this was the most scalable and widely used method, the oldest method for CNT is electric arc discharge and other methods including laser ablation and CVD techniques are different in terms of quality and purity in obtained products TEM images confirms metallic particles are diffused inside the tip of CNTs with the plasma treatment of the catalyst before the growth it is demonstrated with the plasma pretreated catalyst, oxidation of the catalyst is required to induce the base-growth mode. [5].

Laser ablation. A high-power laser vaporizes a graphite target, leading to CNT formation. This method can result in synthesizing SWCNTs with high purity and quality, and this technique has been carried out using several different types of lasers. To determine the quality of the CNT, the processing parameters such as laser power, pulse per point, frequency and speed have been considered. In general, a carbon source, such as graphite, is vaporized in a laser system at specific temperature, pressure and gas environment [5].

1.2. Carbon-Coated Copper

Due to its very high Electrical conductivity (~ 5.4×107 s/m), copper has been considered as a good low-cost conductive filler; therefore, because of its properties, it is a cost-effective alternative to noble metals (silver and gold). Unfortunately, however, CuNPs are very sensitive to oxidation and are typically oxidized to either CuO or Cu_2O which decreases overall electrical conductivity significantly [7, 8].

To deal with this drawback, researchers have developed carbon-coated copper nanoparticles (Cu@C). The carbon coating provides a protective shield over the copper core and prevents the oxidation of the nanoparticles while also protecting the electrical properties of the copper core [8, 7].

Furthermore, the carbon coating enhances the compatibility of the Cu@C nanoparticles with polymer matrices, promoting improved dispersion within epoxy composites [6, 7].

Cu@C based composites typically display relatively low percolation threshold compared to conventional spherical fillers and provide for the efficient formation of conductive networks throughout the composite material. In addition, combining Cu@C nanoparticles with high-aspect-ratio fillers such as carbon nanotubes (CNTs) create strong synergistic effects. For example, CNTs acts as conductive bridges between Cu@C particles and significantly enhance the electrical conductivity of the composites while reducing the percolation thresholds [6].

Thus, hybrid CNT/Cu@C systems process superior electrical performance characteristics and are promising candidates for future application in EMI shielding and advanced electronic devices and components [6].

1.3. Carbonized Nickel

Carbonized nickel or carbon-coated nickel (Ni@C) refers to nickel nanoparticles encapsulated within a carbon shell, forming a core-shell nanostructure. This configuration enhances the stability and functionality of nanoparticles, making them suitable for various applications in catalysis, magnetic properties, and energy storage [9].

An investigation by Narkiewicz et al. [9] demonstrated that carbon-encapsulated metal nanoparticles (CEMNs) could be obtained by the catalytic decomposition of hydrocarbons (CH_4, C_2H_6, C_2H_4) on nanocrystalline nickel. This method results in nickel nanoparticles encapsulated by carbon shells derived from the decomposed hydrocarbons. Nanocrystalline nickel was obtained by precipitation from the nickel nitrate solution, followed by calcination and reduction under hydrogen. A small number of structural promoters (aluminum and calcium oxide) were added to avoid recrystallisation of nickel particles at elevated temperatures. Reduction and carburization of samples were carried out in a differential reactor with mass control. The samples obtained were characterized by using the XRD, SEM and HRTEM methods [9].

Ni@C nanoparticles exhibit several notable properties, such as:

- Catalytic activity. The high surface area and stability of Ni@C nanoparticles make them effective catalysts in various chemical reactions. For example, nickel nanoparticles supported on carbon surfaces have been explored as electrocatalysts for hydrogen evolution reactions [10].

Several methods have been developed for the synthesis of Ni@C nanoparticles:

Carbonization of the loaded and dried resin was treated under the nitrogen over a temperature range of 500-1000 ^{0} C for 2, 4, and 8 h to investigate the effect of temperature and thermolysis time. All eighteen samples prepared were black and contained spherical particles and were attracted by a magnet. The phase composition of synthesized materials was determined using powder X-ray diffraction (PXRD) and Raman spectroscopy. Representative PXRD diffractograms are shown in carbonization temperatures between 500 and 700 ^{0} C, and only FCC-Ni was detected at 800-1000 ^{0}C [11].

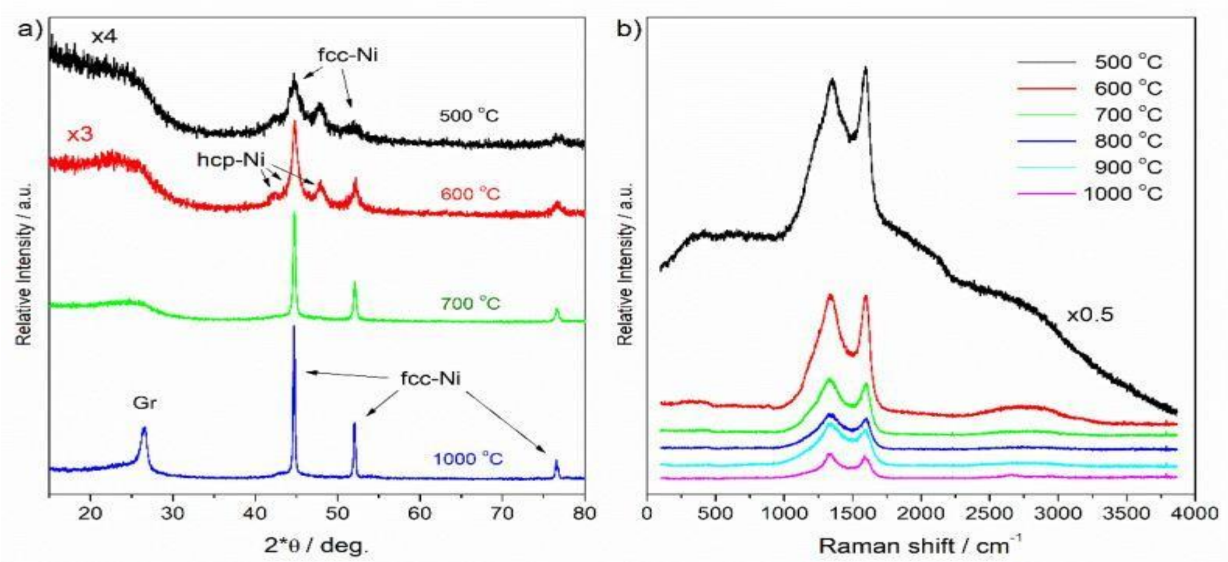

Figure 1.3.1: Powder X-ray diffractogram of selected Ni-NP/C microspheres carbonized for 8 h (b) Raman spectra of Ni-NP/C microspheres for 4 h [11].

According to the scanning electron microscopic (SEM) investigation, the synthesized Ni-NP/C catalysts inherited the spherical morphology of ion exchange resin but shrunk from 600-900 μm (spheres of resin are not uniform) to 300-500 μm due to carbonization.

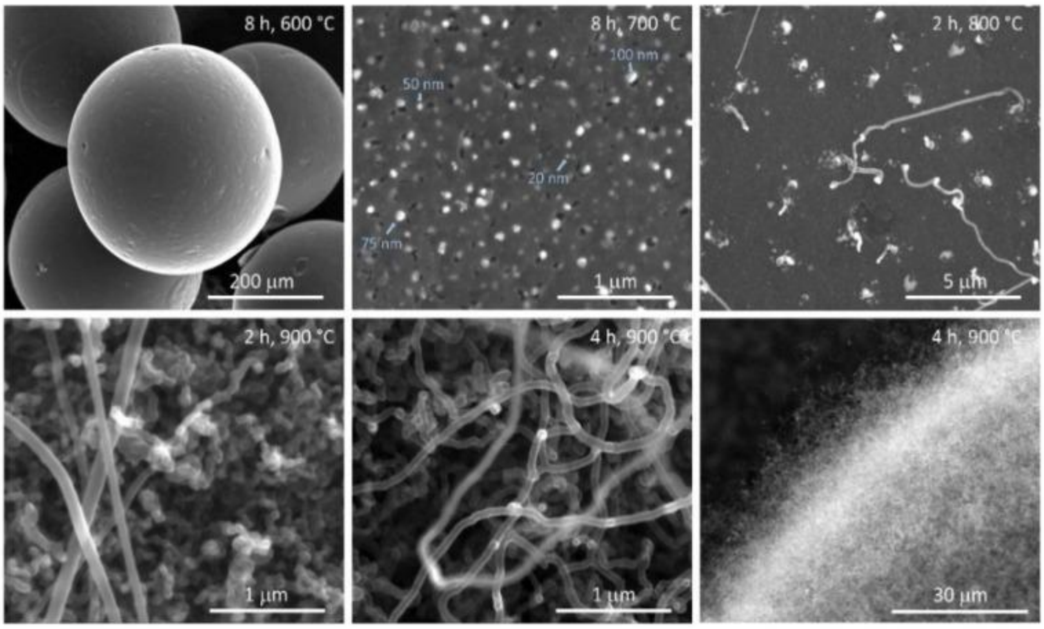

Figure 1.3.2: SEM images of Ni-NP/C [11].

1.4. Carbon Nanotube Composites

Carbon nanotube (CNT) and polymer composites are advanced materials that integrate carbon nanotubes into polymer matrix to enhance the composites properties. Carbon nanotubes are cylindrical structures made of carbon atoms with exceptional, mechanical, electrical and thermal properties. When dispersed within polymers, CNTs can significantly improve the strength, conductivity, and thermal stability of the resulting composite material [12].

These composites are utilized in various applications, including electronics, aerospace and bio medical devices, due to their enhanced performance characteristics. The effectiveness of CNT/polymer composites depends on factors such as the type of CNTs used (single-walled or multi-walled), their dispersion within the polymer matrix, and the nature of the polymer itself [12].

CNT/Polymer composites exhibit several enhanced properties compared to the pure Polymers:

- Mechanical Strength. The addition of CNTs significantly improves tensile strength and the young's modulus. For instance, incorporating 1 wt. % of functionalized SWCNTs into an epoxy matrix increased the young's modulus from 3.27 GPa to 3.49 GPa [13].

- Electrical Conductivity. CNTs impart electrical conductivity to insulating polymers, making these composites suitable for the applications like electromagnetic interference (EMI) Shielding [13].
- Thermal Stability. The thermal conductivity of polymers is enhanced with CNT addition, improving heat dissipation in electronic components [13].

For the composites to work at their best, CNTs must be evenly spread throughout the polymer matrix. This is because well-dispersed CNTs make it easier for the polymer and CNTs to transfer loads, which makes them stronger and more durable [13]. When particles do not spread well, they can stick together and can stress concentration points that make the composite weaker. Uniform distribution also makes it easier for conductive networks to form, which are necessary for the electrical and thermal uses and aggregated CNTs can break up these networks, which makes them less efficient [14].

Chemical functionalization of CNTs, such as adding carboxylic acid groups, enhances their compatibility with the polymer matrix, promoting better dispersion and interfacial bonding. And we can observe two types of functionalization:

- Covalent Functionalization. Functionalization by covalent means making the chemical bonds between functional groups and carbon atoms on the surface of the CNT. This process makes CNTs and the polymer matrix more compatible, which improves how well they mix and stick together at the interface [14].
- Non-Covalent Functionalization. Non-Covalent functionalization relies on physical interactions to disperse CNTs within the polymer matrix without altering their intrinsic structure [14].

There are many ways to make CNT/Polymer composites:

- Mixing by melting. In its molten state, the polymer is mixed with CNTs. This method doesn't Use any solvents, so it can be used on a large scale in factories, but it might cause CNTs to stick together because it is so thick. And it's especially good for thermosetting polymers as the base. This method uses heat and mechanical shearing forces, which are usually found in processes like extrusion and injection moulding [15].
- Polymerization in situ. When dispersed CNTs are present, monomers polymerize, which makes the interface strong and the dispersion even. This approach is especially efficacious for thermosetting polymers [15].
- Solution Processing. The method described here is called solution processing. A polymer and a CNT are dissolved together in solution and then thoroughly mixed. After this process is

finished, the solution is evaporated to manufacture the composite. It provides an excellent distribution of CNTs and is typically utilized as a thin film or coating [15].

1.5. Hybrid Carbon Nanotube Composites

Hybrid composites are made up of two or more types of reinforcing fibers or fillers within a single polymer matrix. The aim is to combine the benefits of each filler and produce a hybrid that has superior qualities compared to other combinations. As an illustration, the use of both microscale carbon fibers (CFs) in conjunction with nanoscale CNTs will result in a composite that takes advantage of the high strength of CFs and the high electrical conductivity of CNTs. The hybrid composites created through hybridization can be designed to suit the specific needs of the application, such as in aerospace, automotive, and electronic industries [16].

Hybrid composites can provide numerous benefits using multiple types of fillers, including the following:

- Increased mechanical properties. The use of multiple fillers can generate mechanical properties that exceed those of single fillers, such as tensile strength, stiffness or toughness. For instance, the combinations of CNTs and GNPs in matrix results in improved tensile and electrical properties of the composite [17].
- Improved thermal and electrical conductivity. Hybrid fillers can provide greater effectiveness in creating conductive pathways for the polymer matrix than did only one filler. This can lead to better thermal management and electrical conductivity in composites [17].
- Custom functionality. Fillers with customized functions can be utilized to design composites that have desired functions, such as Electromagnetic interference (EMI) shielding [17].

Nevertheless, there are also some possible disadvantages to take into mind:

- The complexity of processing. Because of the many fillers that are used, the manufacture of composites with multiple fillers is more complex than those made with a single type of filler, requiring increased levels of control over dispersion and alignment to obtain the desired properties [17, 18].
- Possible filler agitation. Various fillers may be better suited to some types of polymer matrix than others, creating difficulties in achieving uniformly dispersed fillers and causing filler aggregation which can adversely impact composite performance [17, 18].

Synergistic effects may occur in hybrid composites that utilize different types of filler together. A synergy effect in CNT/Polymer composites refers to the state of the sum of the benefits of each filler.

An example of such a synergy effect can occur in a CNT/Polymer composite because of CNT and other nanomaterials/assistant fillers, such as graphene and carbon black [19].

A good example of a synergy effect was demonstrated by Hao et al [18] in which carbon black and multi-wall CNTs were used in conjunction with each other to produce ethylene-propylene-diene rubber (EPDM) composites that exhibited improved mechanical and electrical performance characteristics than the use of just one of these materials. The improvements are the result of materials forming a higher quality conductive network and providing better stress transfer through the composites, producing superior performance characteristics [19].

1.6. Charge Transfer in Carbon Nanotube Composites

Percolation theory is widely used to describe the electrical, thermal and mechanical properties of composite materials. It describes the formation of continuous fillers (like CNTs) increases. In CNT/polymer composites, as the CNT content surpasses a critical threshold, known as a percolation threshold, a network form that allows electrons traverse the material, significantly enhancing its electrical conductivity. This threshold depends on factors such as CNT aspect ratio, dispersion and alignment [20].

In CNT/polymer composites, carrier transport charge occurs primarily through electron tunneling or hopping:

Electron Tunneling. This quantum mechanical process allows electrons to pass through the thin insulating barriers between adjacent CNTs without the need for thermal activation. The probability of tunneling decreases exponentially with increasing distance between CNTs [22].

Electron Hopping. In this thermally activated process, electrons “hop” from one localized state to another, typically over large distances than tunneling. This mechanism becomes more prominent at higher temperatures or when the CNTs are not in proximity [22].

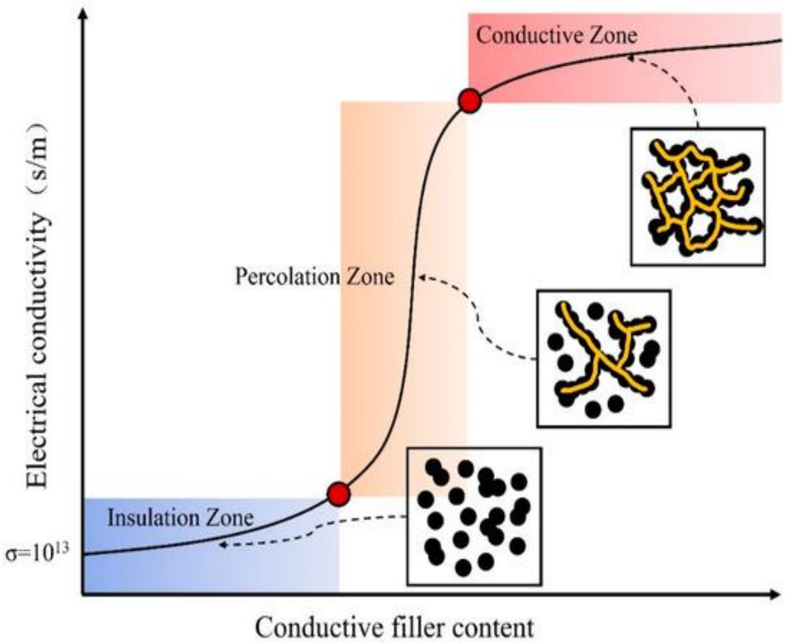

Figure 1.6.1: Conductivity of filled CPCs vs. addition of conductive materials [21].

Lin et al. [24] demonstrate the Zno nanocrystalline films can be described by the VRH and Arrhenius type conduction in electrical transport can be governed by Mott's variable-range hopping mechanism. Electrons cannot move through extended and crystalline structures and are therefore considered to be localized within these structures. The conduction occurs through thermally assisted hopping between these localized states. This is the basis of the hopping model conduction in disordered systems and describes how electrons chose to hop in a manner that maximizes the balance between energy differences and spatial separations and consequently minimizes overall resistance.

The result is characteristic conductivity with respect to the temperature of disordered systems [24]. According to Mott's variable-range hopping model, resistivity is described by the formula:

$$\rho(T) = \rho_0 \exp\left[\left(\frac{T_0}{T}\right)^{\frac{1}{d+1}}\right], \tag{1.6.1}$$

where $\rho(T)$ represents resistivity at a given temperature T, describing how difficult it is for electrons to hop between localized states. The parameter ρ_0 is a constant baseline resistivity, reflecting the material's resistivity in the high-temperature limit. The absolute temperature T controls the hopping probability, while T_0 is the Mott characteristic temperature, which indicates the degree of disorder and localization within the material. Finally, d denotes the dimensionality of the system—whether the hopping occurs in a 1D, 2D, or 3D network—which influences how resistivity varies with temperature.

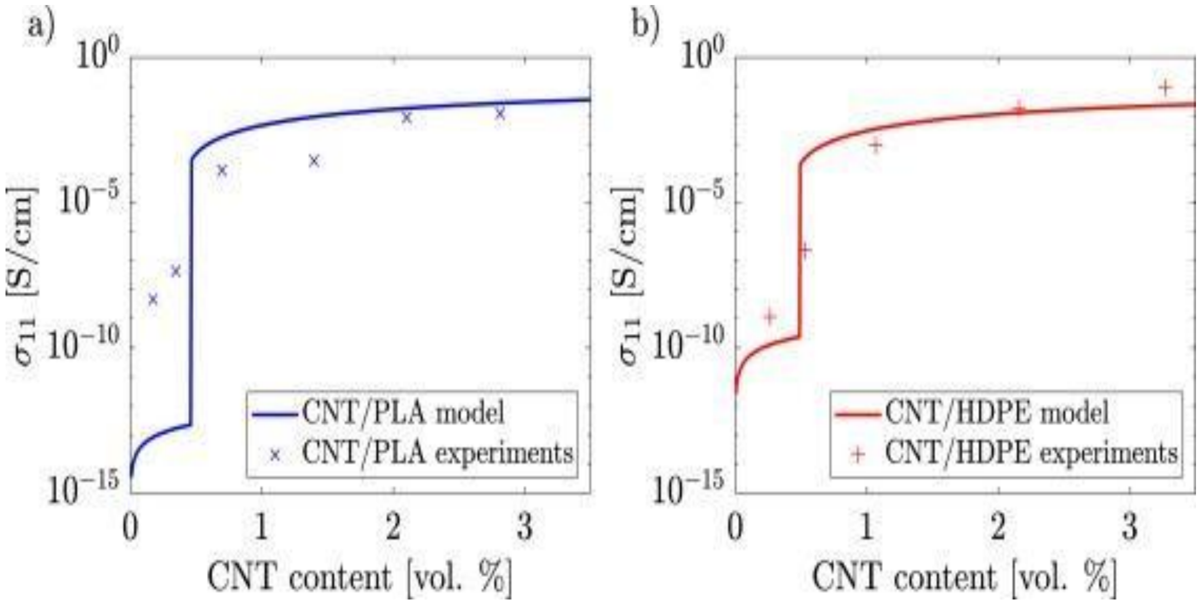

Fig. 1.6.2. Experimental and simulated DC conductivity of (a) CNT/PLA and (b) CNT/HDPE nanocomposites respectively as a function of CNTs volume fraction (vol. %). The solid lines represent the simulated electrical conductivity, while the symbols correspond to the experimental measurements [23].

Processing parameters (such as ultra sonification, purification methods and the fact that surfactants were used to prepare the composites) impact the electrical transport properties of CNT/polymer composites. An excess of ultra sonification or chemical modification may create structural defects, shorten the nanotube lengths and reduce their aspect ratio creates greater carrier localizations. In addition to achieve stable conductive pathways and reduce the percolation threshold. It has been established through experimental investigations that composites with better CNT dispersion will have higher conductivity therefore, this verifies that the morphology of the nanotube network is an important factor that affects electrical transport properties [26].

Lin et al. [24] demonstrate that the electrical transport in nanostructured materials can be effectively described by Arrhenius' thermal activation model. Their results show that charge carriers must overcome an intrinsic energy barrier to contribute to conduction, leading to a strong temperature dependence where conductivity increases with rising temperature. Additionally, other nanostructured systems have exhibited similar thermally activated conduction behavior [25] lending credence to the broader validity of the Arrhenius model for thermally activated transport processes and disordered systems. According to Arrhenius' thermal activation model, conductivity is described by the formula:

$$\sigma(T) = \sigma_0 \exp\left(-\frac{E_a}{k_B T}\right), \tag{1.6.2}$$

where $\sigma(T)$ is the electrical conductivity at temperature T, describing how easily charge carriers can move through the material. The parameter σ_0 is the pre-exponential factor, representing the conductivity in the high-temperature limit. $E_a$is the activation energy, which is the energy barrier that carriers must overcome to conduct, and k_B is the Boltzmann constant. The absolute temperature Tcontrols the fraction of carriers with enough energy to surmount this barrier, so higher temperatures result in higher conductivity.

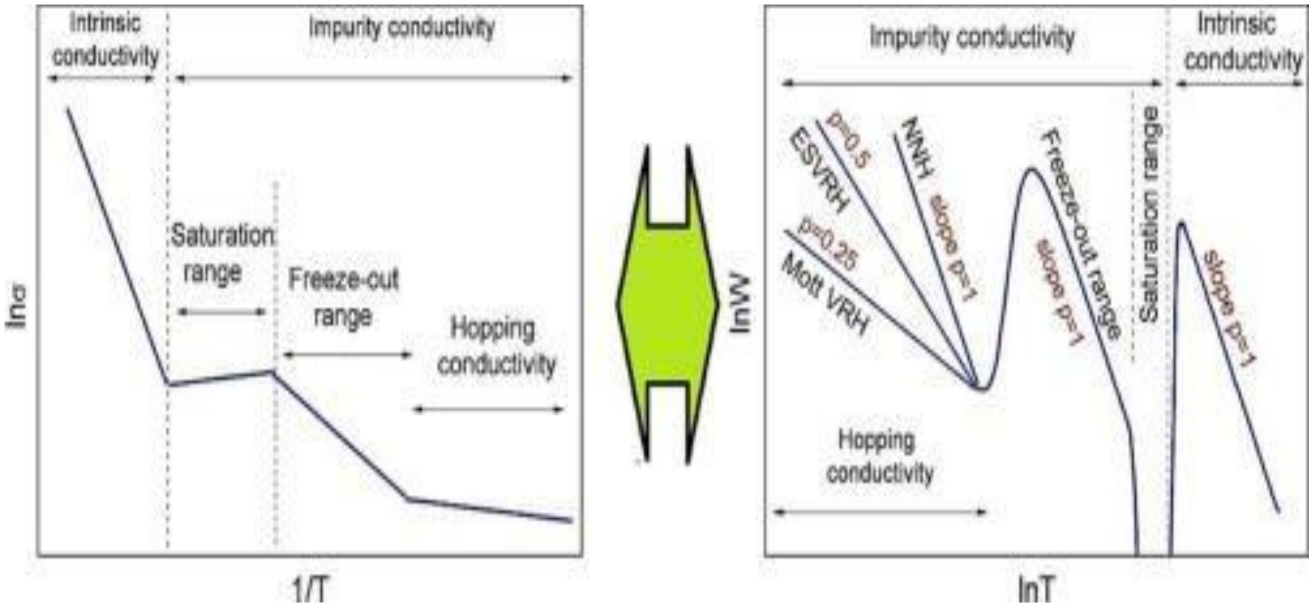

Figure 1.6.3: Conductivity of filled CPCs vs. addition of conductive materials [27].

The conduction mechanism of fluctuation-induced tunneling (FIT) is an established mode of conduction for disordered materials, including CNT-based composites, where conductive regions are separated by thin insulating layers. In CNT -based composites, electronic transport occurs via tunneling of electrons between the conductive domains rather than via continuous metallic conduction CNTs create a localized network of conductive regions (The conductive filler) that are separated by a matrix of insulating material and by air between particles. The tunneling probability between the conductive domains is influenced by the height and breadth of insulating barrier created by the matrix and the gap between conductive particles [28].

The temperature dependence of electrical conductivity due to thermal fluctuations is small (and thus there is little change in the tunneling probability, resulting in higher resistivity). At higher temperatures, the effects of thermal fluctuations become more pronounced, and thermally assisted tunneling becomes the dominant mechanism, resulting in the characteristic temperature dependence in percolative or heterogenous systems [28].

Research has shown that CNT thin film charge transport is dominated by fluctuation induced tunneling. It was indicated that a wide range of temperatures can have charge conduction due to the tunneling of electrons through junctions of CNTs in a disordered way without the addition of other materials. The addition nanoparticles are shown altering the properties of the barriers and conductivity but don't change the overall mechanism of conduction. Using a modified version of the Fluctuation Induced Tunneling model to describe the conductivity's dependence on the temperature for carbon nanofiber thin film materials can provide an understanding of electronic transport in gold doping separations of carbon nanofiber thin film materials [28].

The model's exponential behavior when applied to the experiment may be mathematically written in a more concise manner as stated above:

$$\sigma = \sigma_0 \exp\left(-\frac{T+T_0}{T_1}\right), \tag{1.6.3}$$

Where, σ_0 is the pre-exponential conductivity and T_1 and T_0 characteristic temperatures related to the tunneling barriers and temperature-dependent transport effects.

2. Electric Noise in Carbon Nanotube Composites

This is the second section of the literature review that will focus on different types of noise that can be observed in carbon nanotube composites.

2.1. 1/*f* Noise

1/*f* noise, also known as flicker noise or pink noise, is a type of noise whose power spectral density is inversely proportional to frequency. This means that the noise power increases as the frequency decreases, making it more prominent at low frequencies [29].

1/*f* type noise is present in a wide range of systems, including semiconductors, resistors, biological systems. Its noise power decreases with increasing frequency, unlike white noise, which has a constant power spectral density across all frequencies and because of this, 1/*f* noise becomes significant at low frequencies (< kHz range) and often limits the performance of precision circuits and sensors. Its amplitude distribution is approximately Gaussian, meaning that it follows a bell-shaped curve, and this explains about the low-frequency noise study and the recent developments made in the interpretation and modelling of the low-frequency noise [30].

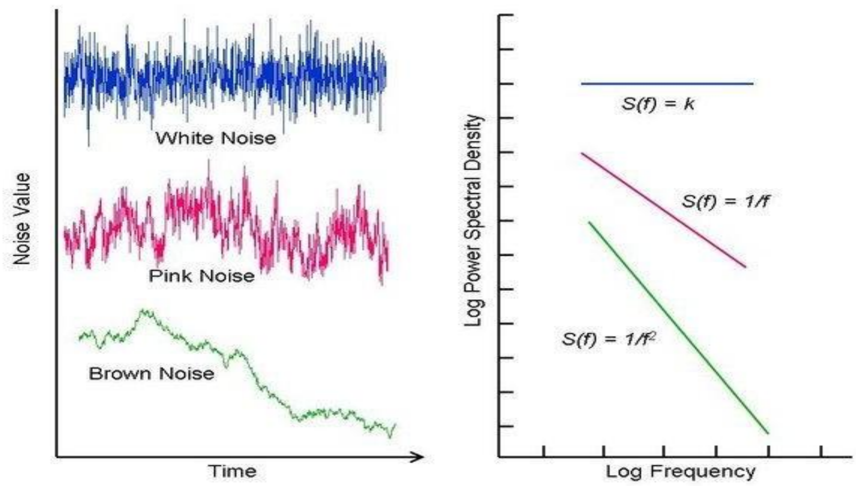

Figure 2.1.1. Flicker noise [31].

1/*f* noise is suggested to have the following origins:

Carrier trapping and de-trapping. Mobility fluctuations occur from impurity scattering or fluctuations of the lattice due to atomic vibrations cause flicker noise, and in metal films, flicker noise is due to primarily to carrier-defect scattering mechanisms. Carrier mobility is an important contributor to flicker noise in GaN-based HEMTs [31].

Defects and dislocations result in structural imperfections in the material. These imperfections produce a fluctuating potential that contributes to low-frequency noise. That early studies on 1/f noise related to defects and impurities later received confirmation through experimental and theoretical models [31].

The equation for describing noise 1/f is given below:

$$S(f) = \frac{K}{f^{\alpha}}, \tag{2.1.1}$$

S(f), which stands for power spectral density, shows that noise powers will tend to become increasingly dominant toward low frequency or 1/f frequencies. In general, the constant α is in a range between 0.8 and 1.2 and therefore close to 1. For example, as frequency decreases, the power increases over time. For a typical power spectral density there is very large amount of 1/f type noise (or low frequency noise) found in most electrical devices and systems including, but not limited to, all types of semiconductor devices and where 1/f noise is often produced due to carrier trapping/de-trapping at defect sites. Other electrical devices that can produce significant amounts of 1/f noise include graphene and other 2D-material based devices where there are also very large amounts of 1/f type frequency/noise fluctuations due to the charge carrier s that can be influenced by adsorbate materials and surficial defects. In addition to producing high amounts of low frequency/1/f-type electrical noise, thin-film-based electrical devices contain a very high ratios of surface area to volume, which generally enhances the impact of carrier trapping, resulting in very high levels of 1/f noise. Finally, low frequency/1/f-type noise is also present in resistive (RRAM) and stable memory devices, whereby the conductive filaments of memory devices can influence the 1/f type noise behavior, potentially causing adverse effects on memory stability [32].

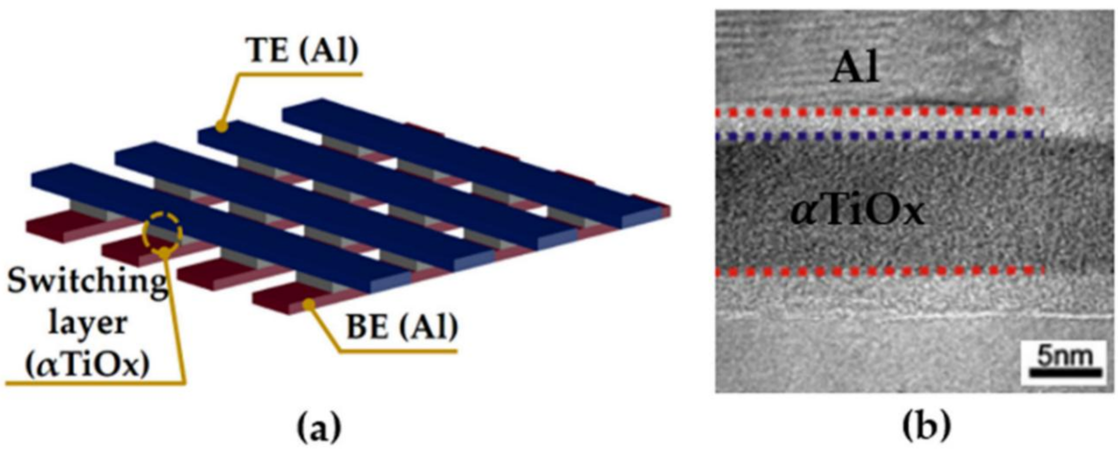

Figure 2.1.2: Shows both the structure of the Al/αTiOx/Al RRAM device as wellas a cross-sectional view from a transmission electron microscope (TEM) [32].

Nah et al. [33] find that low-frequency noise or 1/f is generally seen in many types of materials and there are high levels of 1/f noise due to the trapping and detrapping of carriers at defect centers; Likewise, graphene and other 2D materials display high levels of low-frequency noise due to the influence of surface defects and adsorbed species causing the random fluctuation in charge carriers. Due to their small size and high surface-to-volume ratios.

2.2. Generation-Recombination Noise

The source of G-R noise comes from the electronic noise produced due to the random fluctuations in the generation and recombination of the charge carriers within semiconductor materials. In addition, random fluctuations also occur due to fluctuation in trapping and de-trapping of the charge carriers due to the defects in the semiconductor material. Defining characteristics of G-R noise are as follows:

- Stochastic Process. G–R noise is due to the random fluctuations in the creation and annihilation of charge carriers at defect sites.
- Lorentzian Spectra. G–R noise has a characteristic Lorentzian spectrum, which shows a peak at a certain frequency, and its power spectral density decreases proportionally to the $1/f^2$ [34].

2.3. Thermal Noise

Thermal noise is generated by the random motion of charge carriers (such as electrons) inside any conductor at a non-zero temperature. These random thermal motions cause small, spontaneous fluctuations in voltage and current, even without an external signal. Thermal noise is proportional to the absolute temperature and the resistance of the material. Its power is uniformly distributed over frequency (white noise) and follows a Gaussian distribution:

$$Vn^2 = 4K_B TR\Delta f, \qquad (2.3.1)$$

where in this expression, V_n^2 represents the mean-square thermal noise voltage generated across a resistor. k_B is the Boltzmann constant, 1.38×10^{-23} J/K, and T is the absolute temperature in Kelvin. R denotes the resistance in ohms, while Δf is the bandwidth in hertz over which the noise is measured. This equation describes the thermal (Johnson-Nyquist) noise in resistors, which arises due to the random motion of charge carriers and follows a Gaussian distribution [35].

2.4. Shot Noise

Shot noise arises because electric charge is carried by discrete particles (electrons). And it is observed in PN junction diodes, Schottky diodes, photodiodes and under the steady current flow conditions transistor-based devices. Shot noise exists only when a direct current flows and is not influenced by temperature. It is inherently random, follows a Poisson distribution at its source, and has constant power across frequency (white noise):

$$I_n^2 = 2qI\,\Delta f, \tag{2.4.1}$$

where in this expression, I_n^2 represents the mean-square shot noise current generated by the flow of discrete charge carriers, q is the elementary charge of an electron, 1.602×10^{-19} C, and I is the average DC current that produces the noise. Δf is the bandwidth in hertz over which the noise is measured. This equation describes shot noise, which arises from the discrete nature of charge and is especially significant in devices with low currents or at high frequencies [36].

Shot noise plays a fundamental role in determining the noise floor of many electronic and optoelectronic devices, particularly those operating under low-current conditions. It is commonly observed in the devices such an PN junction diodes, Schottky diodes, photo diodes, vacuum tubes, and field-effect transistors when a steady current flows. In photodetectors, shot noise is directly related to the photocurrent and therefore sets a fundamental limit on the minimum detectable optical signal. Because shot noise is independent of temperature, unlike thermal noise, it cannot be reduced by cooling the device and must instead be mitigated by circuit design strategies such as increasing the signal levels or reducing the bandwidth [36].

3. Studied Sample Characteristics

Composite sample filler concentrations, dimensions and resistivity at 9.12 V are given in Table 3.1. Additionally, this table lists the resistance values for the load resistors used in their study. The role of the load resistor is further described in Section 4 on methodology.

The composite materials examined in this study contain MWCNT and Cu@C fillers in an epoxy matric. As only one type of carbon nanotubes is included in this study, MWCNTs are referred to simply as CNTs.

Table 3.1. Characteristics of composite samples included in this study, and key measurement parameters.

Filler concentration	Surface area, mm^2	Thickness, mm	Resistivity, Ωm (U = 9.12 V)	R_{load}, kΩ
0.05 vol.% CNT + 5 vol.% Cu@C	37.019	3.13	6.89	18.27
0.1 vol.% CNT + 5 vol.% Cu@C	40.61	3.04	3.01	18.27
0.25 vol.% CNT + 5 vol.% Cu@C	44.193	2.98	1.95	18.27
5 vol.% Cu@C	29.37	2.04	356.19	225.5
10 vol.% Cu@C	23.49	2.2	13.5	18.27
15 vol.% Cu@C	21.21	1.7	0.74	6.7

The composite materials were provided by this study by dr. Jan Macutkevič. The studied composite materials consisted of a dielectric polymer matrix with embedded conductive carbon nanoparticles. The samples were prepared by collaborators and delivered in bulk form. These composites were then cut into appropriately sized specimens suitable for electrical measurements. For this research, the type of matrix used was Epikote 828 which is bisphenol -A-based diglycidyl ether of bisphenol A epoxy resin having a density of 1.16 g/cm^3, cured by triethylenetramine (TETA) [6]. The MWCNTs with the diameters ranging from 20 to 40 nm and the lenghths ranging from 0.5 to 200 μm, and were produced using chemical vapor deposition (CVD). The fillers were mixed with isopropanol through ultra-sonification prior to be added to the epoxy resin for uniform mix throughout the matrix of epoxy resin material. After drying any solvent in the composites, they undergo two stages of curing: Stage

1 is curing at room temperature and Stage 2 involves complete cross linking of the resin due to post-curing at high temperatures [6].

Fabrication of epoxy-based nanocomposites with both single filler (Cu@C) and hybrid (CNT/Cu@C) systems at different filler loadings was performed using a multi-step curing and dispersion process that involved the following steps: First, the required amounts of CNT and Cu@C nanoparticles were dispersed in isopropyl alcohol and through the use of ultrasonic dispersion, a uniform suspension was created. The suspension was then mixed with epoxy resin (Component A), and using ultrasonic dispersion, improvements in filler uniformity were achieved. The mixture of fillers and resins was then heated to remove the solvent. The curing agent (Component B) was added in a specified ratio, and after mechanical mixing, the resulting mixture was put into molds for curing at room temperature and post-curing at elevated temperature to achieve fully cross-linked composites. This process facilitates filler uniformity and provides reproducible electrical properties. This fabrication procedure is like previous methods for creating CNT- and Cu@C-based epoxy composites [6].

Nnanoparticles and epoxy are mixed together in a well-stirred state before being ultrasonically agitated to break up agglomarates into a dispersed mixture ready to pour int molds, or cast on to the some type of substrate, and finally cured for polycondensation and hardening of the composite at elevated temperatures (generally 60°C to 120° C).

To create electrical contacts, the composite will then recieve a silver paste applied directly on its surface. The silver paste provides good electrical conductance as well as stable contacts for making future measurements or integrating with devices.

4. Research Methodology

This research looks at how conductive carbon nanoparticles in a polymer-based composite materials produces low-frequency noise and resistance

Measurement Setup and Conditions

All the measurements were performed in a laboratory with shielding to reduce the effect of external electromagnetic interference on the results. The measurement system used was a sample holder with conductive contacts placed inside a chamber with thermal insulation.

Resistance Measurement

The composite resistivity study was performed by measuring the sample voltage using a multimeter Mastech MS8050. Composite resistivity was calculated in reference to the resistance of a known load resistor R_{load}. For resistivity dependence on voltage, different values of constant voltage ranging from 4.5 V to 55 V were applied to the sample at room temperature. For resistivity dependence on temperature in the range of 75 K to 365 K, a fixed voltage of approximately 9.15 V was applied to the sample. A schematic of the experimental setup is shown in Figure 4.1. We can observe the equipment used: a low noise amplifier (LNA), a filter system (F), an analog-to-digital converter (ADC), a personal computer (PC), a reference resistor (R_{ref}), a load resistance (R_{load}).

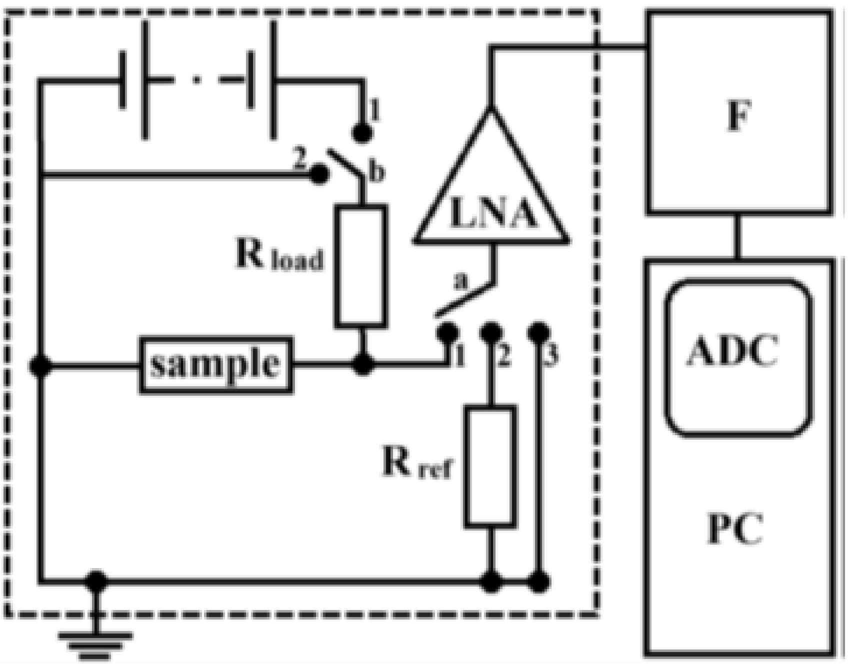

Figure 4.1: Scheme of the noise measuring system [37].

Low-Frequency Noise Measurement

Low-frequency electrical noise was measured in the frequency range of 10 Hz to 20 kHz. A constant DC current was passed through the sample, and the resulting voltage fluctuations (noise) were captured. The signal path included a low-noise amplifier (13 Ω input resistance at 1 kHz), filters, and an analog-to-digital converter (National Instruments PCI-6115). Noise spectra were calculated using a fast Fourier transform (FFT), and the final spectral density was obtained by averaging 200–300 spectra.

Low resistance samples: when the sample resistance allowed the use of a load resistor 10 times higher, the reference resistor (R_{ref}) was used with the circuit switch b in position 1. The spectral density S_U was calculated by:

$$S_U = \frac{U_{\mathrm{ref}}^2 - U_s^2}{U^2 - U_s^2} \cdot 4k_B T R_{\mathrm{ref}}\,, \tag{4.1}$$

where S_U represents the noise spectral density of the sample under test. U^2 is the measured mean-square voltage with the sample connected, while U_{ref}^2 is the mean-square voltage measured with only the reference resistor connected. U_s^2 denotes the mean-square voltage of the measurement system's intrinsic noise (background noise). R_{ref} is the value of the reference resistor, k_B is the Boltzmann constant, and T is the absolute temperature in Kelvin. This formula accounts for the system's background noise to accurately determine the sample's noise characteristics.

High resistance samples: if a 10-fold load resistor was impractical, the measurement used a reference resistor (R_{load}) at least 10 times lower than the sample's resistance, with the switch b in position 2. The noise spectral density was calculated by:

$$S_U = 4k_B T R_{\mathrm{load}} \frac{U_{\mathrm{load}}^2 - U_s^2}{U^2 - U_{\mathrm{load}}^2} \left(\frac{R_{\mathrm{load}} + R}{R_{\mathrm{load}}}\right)^2, \tag{4.2}$$

where S_U represents the noise spectral density of the sample. U^2 is the measured mean-square voltage with the sample connected, while U_{load}^2 is the mean-square voltage measured with only the load resistor. U_s^2 denotes the background noise of the measurement system. R_{load} is the resistance of the load resistor used during the measurement, and $R$is the sample resistance being evaluated. k_B is the Boltzmann constant, and T is the absolute temperature in Kelvin. This formula allows accurate determination of the sample's noise by correcting both the load and the system's intrinsic noise.

5. Results

This section contains the results of resistivity and low frequency noise measurements performed on the MWCNT and Cu@C composite samples, their dependence on the applied voltage and temperature.

5.1 Composite Sample Resistivity Characteristics

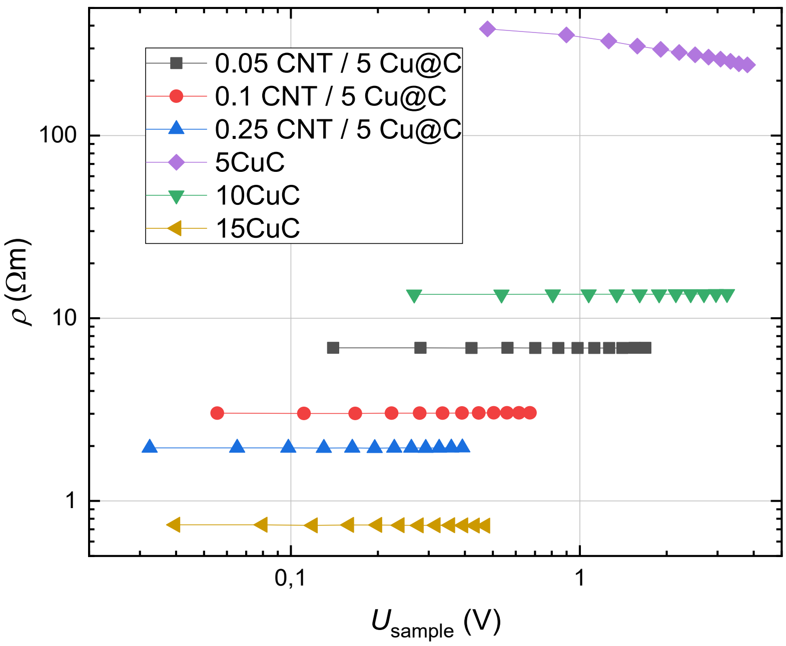

Figure 5.1: Voltage-dependent resistivity of CNT/Cu@C composites at room temperature

Figure 5.1 presents the dependence of electrical resistivity on the applied sample voltage for the composite materials investigated. For nearly all samples, the resistivity remains approximately constant over the studied voltage range, indicating predominantly ohmic or quasi-ohmic conduction behavior. A slight voltage dependence is observed only for the 5 Cu@C sample, where resistivity shows a more noticeable variation compared to the other composites.

Overall, the weak dependence of resistivity on voltage indicates that field-assisted transport mechanisms are not dominant, and charge transport is primarily governed by percolation through conductive networks formed by the fillers. At room temperature conduction in such composites is typically controlled by electron transport along interconnected conductive pathways, with possible minor contributions from tunneling between adjacent filler particles.

A comparison between different compositions reveals that resistivity strongly depends on filler type and concentration. In hybrid composites (0.05 CNT/5 Cu@C, 0.1 CNT/5 Cu@C, 0.25 CNT/5 Cu@C), all samples exhibit relatively low resistivity values with only small differences between them. This indicates that even at low CNT concentrations, a well-developed conductive network is already established, enabling efficient transport charge.

It is also worth noting that although the amount of CNT used in the 0.05 CNT/5 Cu@C composite is two orders of magnitude less than that used in the 10 Cu@C composites, the resistivity of these two composites is almost identical. This shows that CNTs are much better at establishing conductive pathways than Cu@C fillers, this behavior is likely due to the CNTs extremely high aspect ratio, which allows for earlier percolation and more effective formation of CNT networks compared to low-aspect-ratio spherical Cu@C particles. As a result, a small amount of CNTs effectively replaces a larger quantity of Cu@C with almost the same resistive characteristics.

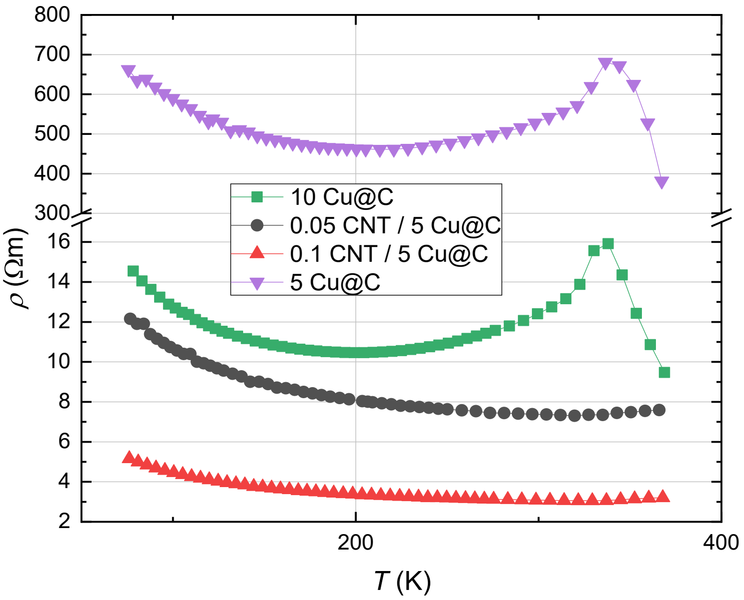

Figure 5.2: Composite sample resistivity dependence on temperature ($U = 9.12$ V).

According to Figure 5.2, the resistivity values for each composite material are decreasing with increases in temperature throughout most of the temperature range. The decrease in resistivity provided evidence that these composites have a mechanism for transporting electronically charged carriers that are thermally activated.

In addition, the Cu@C- based composites (single-filler composites) have non-monotonic temperature dependencies for their resistivity values. For the Cu@C composites, resistivity begins to drop at relatively low temperatures and reaches a minimum value at ~ 200 K. After ~ 200 K, resistivity begins to increase as temperatures rise until reaching ~335 K. Above ~335 K, the resistivity of these composites decreases rapidly. This temperature-dependent behavior is taught to be related to both structural and interparticle effects that occur as a result of temperature in these composites. Specifically, the increase in resistivity between ~200 K and ~335 K may be due to the thermal expansion of polymer matrix, which creates greater separation between particles and disrupts the conductive pathways within the composite. Conversely, the rapid decrease in resistivity near ~ 335 K suggests that the polymer matrix has achieved sufficient thermal activation to facilitate an increase in the amount of charge transported through the matrix itself.

Contrary to other systems, CNT containing composites exhibits a more stable and low resistivity throughout the entire range of temperature. This suggests that there are better pathways for charge transport as CNTs enhance the interconnectivity between conductive regions (Cu@C) and limit the sensitivity of the system to thermally induced structural changes. This could again be related to the higher aspect ratio of CNTs, which can then act as conductive bridges between the lower aspect ratio spherical Cu@C particles.

In summary, data suggests that CNTs alter the temperature response of the composite through stabilization of the conductive network and reducing matrix expansion effect on electrical transport. Conversely, single-filler Cu@C composites are more sensitive to the effects of thermal expansion, as well as the emergence of electric conductivity in the epoxy matrix itself at high temperatures.

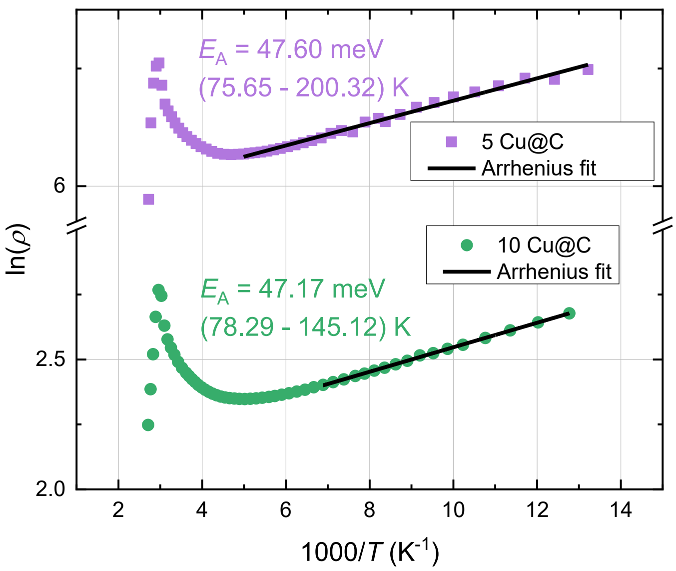

Figure 5.3: Arrhenius plot of the resistivity ln(ρ) as a function of inverse temperature. Dots are experimental data; lines are the Arrhenius fit.

To identify the charge carrier transfer mechanisms in these composites, mathematical modelling of the resistivity dependence on temperature was performed. Figure 5.3 shows the Arrhenius plot of electrical resistivity of single-filler Cu@C composites. The plot shows the ln(ρ) as the function of inverse temperature (1000/T). The symbols represent the experimental data, and straight lines represent the linear fit in high temperature region.

The linearity at lower 1000/T (inverse temperature region) confirms that the conduction mechanism is of Arrhenius-type thermally activated transport. In this regime, charge carriers acquire sufficient thermal energy to surmount potential barriers and conduct by means of hopping between localized states.

The activation energy E_A is calculated from the slope of linear regions is removed. The obtained values (~47 meV) point towards mechanism of thermally activated hopping processes for carrier transport in composite and observe that the activation energy is slightly lower for the 10 Cu@C composites

At higher temperatures (low 1000/T) a deviation from linearity observed indicating a breakdown of the Arrhenius behavior. This deviation indicates that thermally activated hoping is no longer the dominant mechanism and tunneling processes start to dominate the charge transport.

The similar activation energies for different samples indicate that the energy barriers for transport charge are similar, whereas the minor differences suggest differences in the connectivity of the conductive network. Improved connectivity lowers the energy effective barrier and promotes the charge of transport.

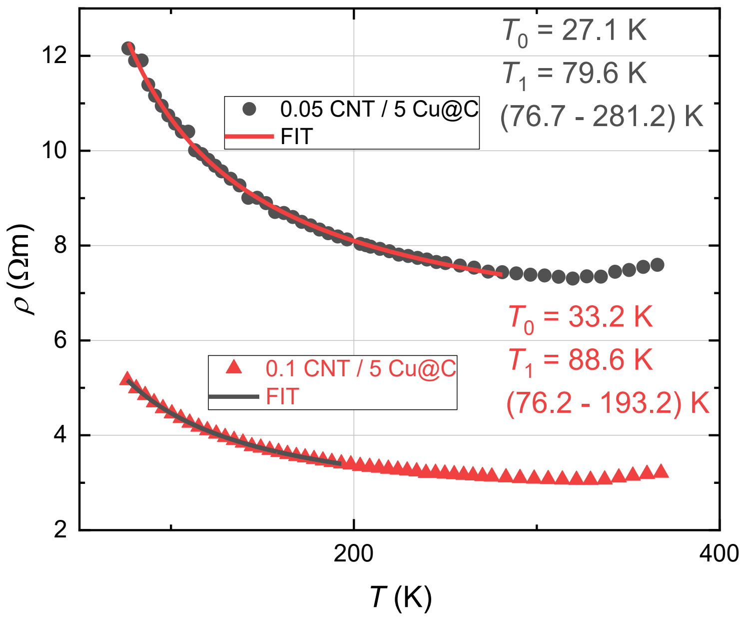

Figure 5.4: Temperature dependence of resistivity fitted using the Fluctuation induced tunneling (FIT) Model for CNT/Cu@C Composites.

The figure 5.4 illustrates how the temperature affects the resistivity of the CNT/Cu@C composites for different amounts of CNTs. Each data point on the X-axis is the measured value, while the solid lines provide mathematical fit of the FIT model to those measured points.

The resistivity is high at low temperatures because of the limited number of charge carriers that can transport across the gaps between conductive regions. At this temperature range, conductive CNT pathways are separated by thin insulating gaps and charge carriers will have to tunnel through the barriers to reach the other side. However, the thermal energy at this point is low enough that there will not be enough charge carriers available to tunnels, resulting in a high level of resistivity.

When an increase in the temperature is experienced, the thermal fluctuations allow for a more extensive range of charge carriers to tunnel through the barriers separating conductive CNT pathways is gradually decreased. This indicates that the conductivity of conductive CNT pathways is controlled by an increase in thermally assisted tunneling processes.

Based on the fitted curves and experimental data, tunneling through fluctuations (FIT) is responsible for most conduction of the hybrid CNT/Cu@C composites in the given temperature ranges. As the temperature rises, resistivity decreases at a slower rate, which means that more stable routes for conduction are being formed and thermal changes will have decreased the effects of these fluctuations on the conductivity of composite. The FIT model uses the T_0 and T_1 parameters of the tunneling pathway as the basis for the determination of the tunneling mechanisms. The first parameter, T_0 is also related to how much energy will be lost during the tunneling, where higher T_0 indicates that the barrier will require a large amount of thermal energy to allow the electrons to tunnel through the barrier, and lower T_0 indicates that barrier requires less energy. T_1 represents the scale at which thermal fluctuations can assist electron tunneling; therefore, higher values of T_1 indicate that conductivity will depend more on temperature, while lower values for T_1 indicate that the conductive paths are more stable and will have less temperature dependence.

Finally, the results are consistent with the notion that the conductivity of CNT/Cu@C composites is achieved by tunneling through conductive networks and that these conductive networks are subjected to fluctuation-based effects that are dependent on temperature.

5.2. Composite Sample Low Frequency Noise Characteristics

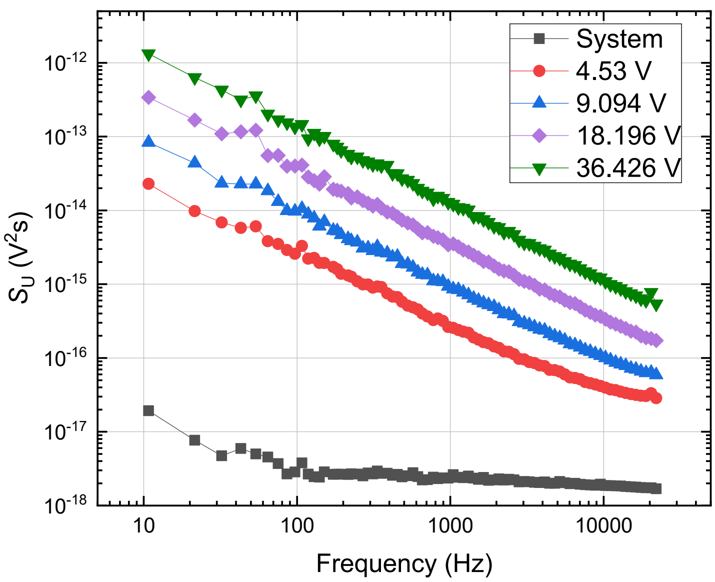

Figure 5.5: Characteristic noise spectra for a 10 vol.% Cu@C composite at room temperature.

Characteristic noise spectra for the 10 Cu@C composites, reflective of the noise spectra observed during the study for all composites, are given in Figure 5.5 (voltage dependency case) and Figure 5.6 (temperature dependency case). The noise spectra demonstrate a clear characteristic 1/f dependence over a broad range of frequencies, which is the fingerprint of flicker noise, the existence of flicker noise expected from the disordered nature of the CNTs and the carrier transport mechanisms of charge carriers through hopping and tunneling between the potential barriers within the composite network. The presence of 1/f dependency in the noise spectra of the composite material demonstrates that the resistance fluctuations are dependent upon the intrinsic material disorder of the CNTs and the dynamics of carrier transport.

The upward shift of the total spectra increasing with the applied voltage indicates that the degradation of the noise characteristics results in the increase in the amount of noise produced. This data implies the transport of charges under high electric fields are dependent upon the degree of noise present and the result from the increased charge injection by the carriers, increased conduction due to trap-assisted mechanisms and activation of additional conductive pathways in composite materials.

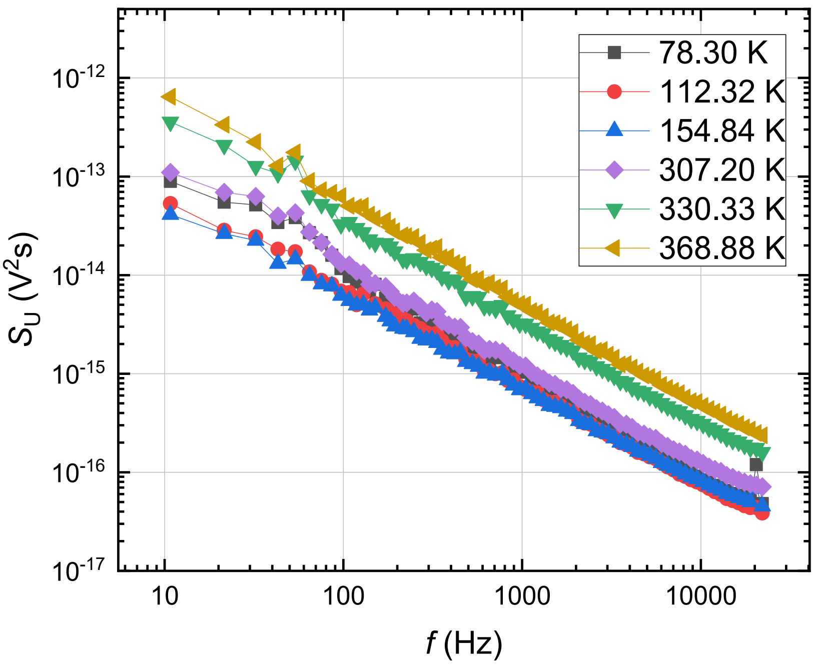

Figure 5.6: Characteristic noise spectra for a 10 vol.% Cu@C composite at various temperatures ($U = 9.12$ V).

Characteristic noise spectra for the 10 vol.% Cu@C composite at different temperatures using a constant applied voltage is shown in figure 5.6. The spectra exhibit a clear 1/f dependence over the entire frequency range, which suggests that the dominant noise mechanism does not change with temperature. Distinct generation-recombination noise spectra (Lorentzian peaks) were not observed. Therefore, it can be concluded that the noise is not caused by singular defects with specific characteristic times, but many generation-recombination centers with varying characteristic times that average out into $1/f$ type noise.

When the temperature increases, the noise spectral density magnitude also increases. Lower noise levels are associated with lower temperature due tot he fact that rate of carrier mobility and the thermal fluctuations have been reduced. Higher thermal energies create additinal carrier excitation and increas the rate of scattering, therefore increasing the fluctuations in the conductivity. This these results supports a thermally activated transport mechanism and imply a graeter degree of interaction of charge carriers with defects or localized states within the composite material.

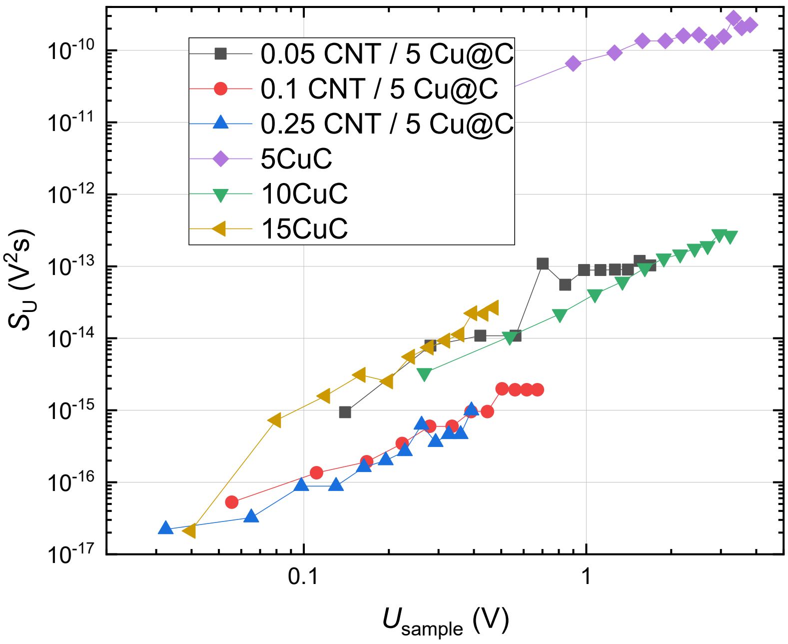

Figure 5.7: Spectral density dependence on voltage at fixed frequency (107 Hz, room temperature).

Figure 5.7 shows (voltage noise spectral density) sample voltage for composites tested at fixed frequencies. The voltage noise results indicate then level of noise is affected by the composition of composite materials and the structure of conductivity network.

Of the single-filler composites, 5 Cu@C shows the greatest noise level, which is indicative of a poorly connected and unstable conductive network. As the amount of copper in the hybrid composites increases from 10 Cu@C to 15 Cu@C, there is a significant drop in the level of noise present indicating there was an increase in the quality and stability of the electrical connection points within the composite films. The composite materials that have Cu@C concentration of 10 Cu@C had the most stable and nearly linear response, which implies that composite had developed into an excellent electrically conductive network.

The hybrid composite films that have the CNT inclusions (0.05 CNT/5 Cu@C, 0.1 CNT/5 Cu@C, 0.25 CNT/5 Cu@C) showed lower noise levels than the composites without CNTs in their construction. The increase in CNT concentration had a significant impact on improving the electrical characteristics of composite films through the addition of CNT materials.

The differences between hybrid samples are relatively small, indicating that even low CNT concentrations are sufficient to significantly enhance conductive network formation. In particular, the 0.05 CNT/5 Cu@C sample shows noise levels comparable to, or slightly lower than, those of 10 Cu@C sample, confirming that a small addition of CNTs can effectively replace a significant increase in Cu@C content while maintaining similar electrical characteristics.

The observed noise behavior follows a power-law relationship:

$$S_U \propto U^b$$

where the exponent b provides insight into the dominant charge transport mechanisms. To facilitate this analysis, presents the normalized quantity S_U/U^2, where a horizontal trend corresponds to an exponent value of $b \approx 2$, indicating noise dominated by resistance fluctuations.

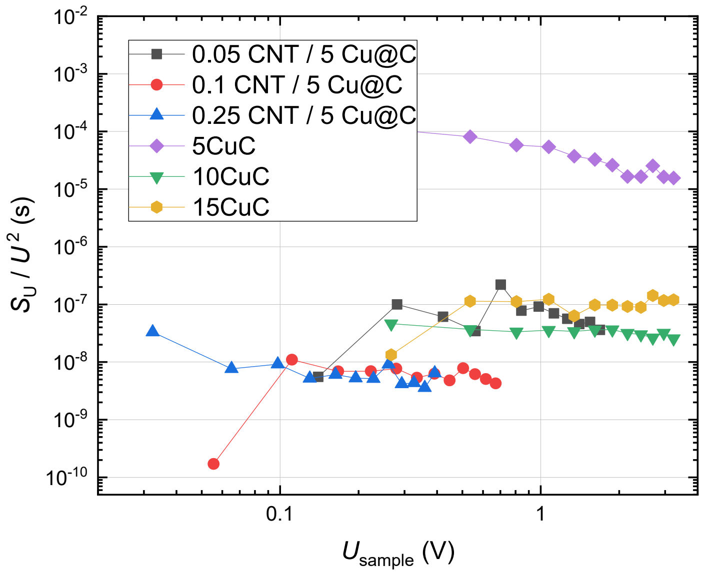

Figure 5.8: Voltage dependence of normalized noise spectral density at fixed frequency (107 Hz).

From the figure 5.8, most samples show a weak dependence of normalized noise (S_U/U^2) on voltage, with nearly flat or slightly varied trends. This indicates that the exponent b is close to 2, meaning the noise is mainly governed by the resistance fluctuations within the conductive network that is more sensitive to external electric fields, likely due to an incomplete or poorly developed percolation structure.

In contrast, the 10 Cu@C and 15 Cu@C composites display lower and more stable S_U/U^2 values with almost no voltage dependence. This behavior indicates the formation of stronger, well-connected conductive networks where charge transport is more uniform. Thus, these noise characteristics are predominantly due to fluctuations in the intrinsic resistances of the connections in the networks, rather than due to barrier limited or tunneling effects; indicating improvements in the structural homogeneity and stability of the networks.

For the hybrid composites (0.05 CNT/5 Cu@C, 0.1 CNT/5 Cu@C, 0.25 CNT/5 Cu@C), all show the level of normalized noise with low voltage dependence; indicating very efficient and stable transport through the networks. The small amount of variation among the hybrids indicates that even small concentrations of CNTs can provide significant bridge between adjacent conducting particles improving connectivity of the network as a whole and resulting in greater total charge transport through the entire composite. With the incorporation of changes in the filler percentage and addition of CNT provide greater stability in the conductive network, lower total noise levels, and facilitate the transport through the conductive networks by allowing for continuous percolation paths rather predominantly tunnel mechanism transport, which would be more susceptible to fluctuations in the performance of network.

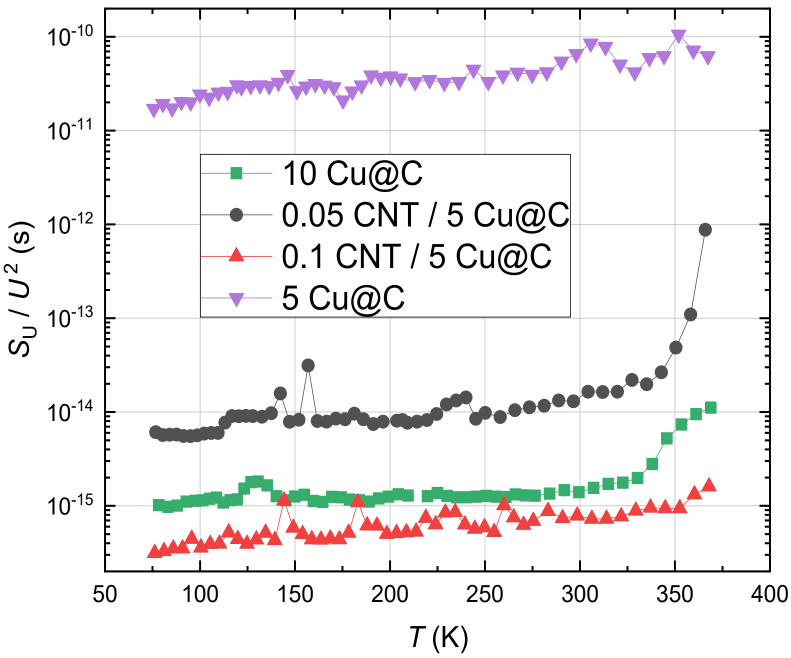

Figure 5.9: Normalized noise (S_U/U^2) in relation to temperature (T) (107 Hz, U = 9.12 V).

It can be seen from figure 5.9 that as the temperature increases, the normalized noise (S_U/U^2) for each of the samples also increases, which shows that there is a significant thermal effect on the fluctuations of the resistance. The low temperatures have correspondingly low levels of noise because there are fewer charge carriers available to contribute to the motion and scattering that produce noise, while at higher temperatures there are increased number of charge carriers and hence higher levels of nosie due to their increased thermal energy which causes greater motion and scattering of those charge carriers.

The noise level for the tested samples was highest for the 5 Cu@C composites among the tested composite groups. This higher level of noise corresponds among the tested composite groups. This higher level of noise corresponds with a higher resistivity which points to less efficient charge transport in the composite conductive network. The noise characteristics for the 10 Cu@C composites were less variable and showed the lower levels of noise. These findings suggest that the electrical conduction in this sample was improved from the creation of a more complete and effective percolation path for charge transport in the composite structure.

For the hybrid composites (0.05 CNT/5 Cu@C, 0.1 CNT/5 Cu@C), noise levels are low and relatively stable across the temperature range. This indicates that CNTs improves network connectivity by bridging gaps between Cu particles, reducing fluctuations. Overall, hybrid systems and optimized filler loading result in improved stability and reduced noise.

Conclusions

1. Hybrid CNT/Cu@C composites have generally lower resistivity than single-filler Cu@C composites at comparatively lower total filler concentration, indicating the superior capability of CNTs to aid in the formation of a conductive network within the composite due to their higher aspect ratio.
2. The temperature dependence of resistivity depends on the type of filler in the composite. The resistivity of single-filler Cu@C composites is more strongly affected by the thermal expansion of the matrix.
3. Charge carrier transport in the CNT/Cu@C composites is thermally activated, described by the Arrhenius model for single-filler Cu@C composites in the temperature range of 75 K – 145 K, and fluctuation induced tunneling model for the hybrid CNT/Cu@C composites in the temperature range of 75 K – 193 K.
4. In the low frequency range (10 Hz – 20 kHz), all composites were found to exhibit $1/f$ type noise. In single-filler Cu@C composites with higher concentrations of filler (10, 15 vol.% Cu@C), the noise level is proportional to the voltage square, and is due to fluctuations of resistance. For the remaining composites, noise level is proportional to the voltage, and is due to a higher presence of tunneling. The hybrid composite materials have lower normalized noise level than the single-filler Cu@C composites.

Vilniaus universitetas Fizikos fakultetas
Taikomosios Elektrodinamikos ir Telekomunikacijų institutas

Vakada Venkata Sai Mohan Revanth

Kompozitų su anglies nanodalelėmis žemo dažnio triukšmo charakteristikos

Magistro baigiamasis darbas

Santrauka

Šio darbo tikslas yra ištirti epoksidinės dervos matricos kompozitų su daugiasienių anglies nanovamzdelių (CNT) ir anglimi dengto vario nanodalelių (Cu@C) užpildais varžines ir žemo dažnio triukšmo charakteristikas.

Savitosios varžos ir žemo dažnio triukšmo (10 Hz – 20 kHz) tyrimai atlikti kambario temperatūroje, įtampos intervale nuo 4,5 V iki 55 V, bei keičiant kompozitinio bandinio temperatūrą intervale nuo 75 K iki 365 K esant pastoviai 9,12 V įtampai. Tiriami vienfaziai Cu@C bei daugiafaziai CNT/Cu@C kompozitai su skirtingomis užpildų koncentracijomis.

Kompozitų savitoji varža priklauso nuo užpildų tipo ir koncentracijos. Kompozitų su didesnėmis užpildų koncentracijomis savitoji varža yra mažesnė. Daugiafazių CNT/Cu@C kompozitų savitoji varža yra mažesnė nei vienfazių Cu@C kompozitų esant palyginamai mažesnėms užpildų koncentracijoms dėl didesnio CNT kraštinių santykio. Taip pat, vienfazių Cu@C kompozitų savitoji varža labiau priklauso nuo matricos šiluminės plėtros.

Krūvio pernaša tiriamuose kompozituose yra termiškai aktyvuotas procesas. Kompozitų su Cu@C užpildais savitosios varžos priklausomybei nuo temperatūros intervale nuo 75 K iki 145 K taikytinas Arenijaus šiluminės aktyvacijos modelis. Kompozitų su CNT ir Cu@C užpildais savitosios varžos priklausomybei nuo temperatūros intervale nuo 75 K iki 193 K taikytinas fliuktuacijų sukelto tuneliavimo modelis.

Tiriamajame dažnių intervale nuo 10 Hz iki 20 kHz, kompozitų žemo dažnio triukšmas yra 1/f tipo. Vienfazių kompozitų su 10 ar 15 vol.% Cu@C triukšmo lygmuo yra proporcingas įtampos kvadratui, kas yra būdinga triukšmui, kylančiam dėl varžos fliuktuacijų. Likusių kompozitų triukšmo lygmuo yra proporcingas įtampai, kas sietina su žymesniu tuneliavimo reiškinių indėliu.

Vilnius University Faculty of Physics

Institute of Applied Electrodynamics and Telecommunications

Vakada Venkata Sai Mohan Revanth

Low-frequency Noise Characteristics of Composites with Carbon Nanoparticles

Mater's thesis

Summary

The aim of this work is to investigate the resistive and low-frequency noise characteristics of epoxy resin matrix composites with multi-walled carbon nanotubes (CNT) and carbon-coated copper nanoparticles (Cu@C) fillers.

Resistivity and low-frequency noise (10 Hz – 20 kHz) studies were performed at room temperature, in the voltage range from 4.5 V to 55 V, and by changing the temperature of the composite sample in the range from 75 K to 365 K at a constant voltage of 9.12 V. Single-phase Cu@C and multi-phase CNT/Cu@C composites with different filler concentrations were studied.

The resistivity of the composites depends on the type and concentration of fillers. Composites with higher filler concentrations have lower resistivity. Multi-phase CNT/Cu@C composites have lower resistivity than single-phase Cu@C composites at comparatively lower filler concentrations due to the higher CNT aspect ratio. Also, the resistivity of single-phase Cu@C composites is more dependent on the thermal expansion of the matrix.

Charge transfer in the studied composites is a thermally activated process. The Arrhenius thermal activation model is applicable to the temperature dependence of the resistivity of the composites with Cu@C fillers in the range from 75 K to 145 K. The fluctuation-induced tunneling model is applicable to the temperature dependence of the resistivity of composites with CNT and Cu@C fillers in the range from 75 K to 193 K.

In the investigated frequency range from 10 Hz – 20 kHz, the low-frequency noise of the composites is of the 1/f type. The noise level of the single-phase composites with 10 or 15 vol.% Cu@C is proportional to the square of the voltage, which is characteristic of noise arising from impedance fluctuations. The noise level of the remaining composites is proportional to the voltage, which is associated with a more significant contribution of tunneling phenomena.

References

[1] Mireckas, F., Meisak, D., Pralgauskaitė, S., Macutkevič, J., Matukas, J., & Banys, J., "Low-frequency noise and resistivity of hybrid MWCNT/Ni@C/epoxy composites," Fluctuation and Noise Letters, 2025, doi: 10.1142/S0219477525400188.

[2] Segale, M., Seadira, T., Sigwadi, R., Mokrani, T., & Summers, G., "A new frontier towards the development of efficient SPEEK polymer membranes for PEM fuel cell applications: A review," Materials Advances, vol. 5, pp. 7979–8006, 2024, doi: 10.1039/D4MA00628C.

[3] K. Kumar, D. Narnolia, R. Raj, P. K. Jain, and K. Kumar, "Computational investigation on ablation kinetics of graphene and carbon nanotube reinforced thermoset polymeric composites," International Journal on Interactive Design and Manufacturing (IJIDeM), vol. 19, no. 9, pp. 6361–6371, Sep. 2025, doi: 10.1007/s12008-024-02208-z.

[4] Z. Ali, S. Yaqoob, J. Yu, and A. D'Amore, "Critical review on the characterization, preparation, and enhanced mechanical, thermal, and electrical properties of carbon nanotubes and their hybrid filler polymer composites for various applications," Composites Part C: Open Access, vol. 13, p. 100434, 2024, doi: 10.1016/j.jcomc.2024.100434.

[5] Yahyazadeh, A., Nanda, S., & Dalai, A. K. Carbon Nanotubes: A Review of Synthesis Methods and Applications. Reactions, 2024, 5(3), 429–451. doi: 10.3390/reactions5030022

[6] D. Tsyhanok, D. Meisak, J. Banys, J. Macutkevič, A. Selskis, A. Sabalina, O. Platnieks, and S. Gaidukovs, "Dielectric spectroscopy and synergistic effects in epoxy composites filled with multi-walled carbon nanotubes and carbon-coated copper nanoparticles," Polymer Composites, vol. 46, pp. 5994–6007, 2025, doi: 10.1002/pc.29337.

[7] M. C. Crisan, M. Teodora, and M. Lucian, "Copper nanoparticles: synthesis and characterization, physiology, toxicity and antimicrobial applications," Applied Sciences, vol. 12, p. 141, 2022, doi: 10.3390/app12010141.

[8] J. Chen, H. Y. Zhang, X. P. Liu, and L. P. Li, "Synthesis and Antioxidant Behavior of Carbon Coated Copper Nanoparticles," AMR, vol. 568, pp. 299–302, Sep. 2012, doi: 10.4028/www.scientific.net/amr.568.299.

[9] U. Narkiewicz and M. Podsiadły, "Synthesis of carbon-encapsulated nickel nanoparticles," Applied Surface Science, vol. 256, no. 17, pp. 5249–5253, 2010, doi: 10.1016/j.apsusc.2009.12.112.

[10] Kannan Gothandapani, R.; Jeniffer, R.S.; Selvi, G.T.; Velmurugan, V.; Assaifan, A.K.; Alzahrani, K.E.; Albrithen, H.; Muthuramamoorthy, M.; Pandiaraj, S.; Pitchaimuthu, S.; Alodhayb, A.N. Grace, A.N. Nickel nanoparticles supported on carbon surface as an electrocatalyst for hydrogen evolution reaction. International Journal of Hydrogen Energy 2024, 52, 1137–1146. doi: 10.1016/j.ijhydene.2023.08.027

[11] M. Krebsz, L. Kótai, I. E. Sajó, T. Váczi, and T. Pasinszki, "Carbon microsphere-supported metallic nickel nanoparticles as novel heterogeneous catalysts and their application for the reduction of nitrophenol," Molecules, vol. 26, p. 5680, 2021, doi: 10.3390/molecules26185680.

[12] Andrews, R.; Weisenberger, M.C. Carbon nanotube polymer composites. Curr. Opin. Solid State Mater. Sci. 2004, 8, 31–37. doi: 10.1016/j.cossms.2003.10.006

[13] Yim, Y.-J.; Yoon, Y.-H.; Kim, S.-H.; Lee, J.-H.; Chung, D.-C.; Kim, B.-J. Carbon Nanotube/Polymer Composites for Functional Applications. Polymers 2025, 17, 119. doi: 10.3390/polym17010119

[14] Mohd Nurazzi, N.; Asyraf, M.R.M.; Khalina, A.; Abdullah, N.; Sabaruddin, F.A.; Kamarudin, S.H.; Ahmad, S.; Mahat, A.M.; Lee, C.L.; Aisyah, H.A.; et al. Fabrication, Functionalization, and Application of Carbon Nanotube-Reinforced Polymer Composite: An Overview. Polymers 2021, 13, 1047. doi: 10.3390/polym13071047

[15] Lim, J.-V.; Bee, S.-T.; Tin Sin, L.; Ratnam, C.T.; Abdul Hamid, Z.A. A Review on the Synthesis, Properties, and Utilities of Functionalized Carbon Nanoparticles for Polymer Nanocomposites. Polymers 2021, 13, 3547. doi: 10.3390/polym13203547

[16] Abdul Raheem, K. M., & Subbaya, K. Performance Evaluation of Hybrid Polymer Composite Materials in Marine Applications: A Review. Materials Today: Proceedings, 2023. doi: 10.1016/j.matpr.2023.01.346

[17] Zhang, H., Huang, Y., Jiang, Q., & Zhang, J. Synergistic Effect of Carbon Nanotube and Graphene Nanoplates on the Mechanical, Electrical and Electromagnetic Interference Shielding Properties of Polymer Composites and Polymer Composite Foams. Chemical Engineering Journal, 2018, 353, 381–393. doi: 10.1016/j.cej.2018.07.144

[18] Hao, Y., He, X., Sun, X., & Zhou, X. The Influence of Multiple Fillers on Friction and Wear Behavior of Epoxy Composite Coatings. Surface and Coatings Technology, 2019, 362, 213–219. doi: 10.1016/j.surfcoat.2019.01.110

[19] Kang, H.; Bae, J.; Lee, J.; Yun, Y.; Jeon, S.; Chung, N.; Jung, J.; Baek, U.; Lee, J.; Kim, Y.; et al. The Synergistic Effect of Carbon Black/Carbon Nanotube Hybrid Fillers on the Physical and Mechanical Properties of EPDM Composites after Exposure to High-Pressure Hydrogen Gas. Polymers 2024, 16, 1065. doi: 10.3390/polym16081065

[20] Monajjemi, M., Baheri, H., & Mollaamin, F. A Percolation Model for Carbon Nanotube-Polymer Composites Using the Mandelbrot-Given Curve. Journal of Structural Chemistry, 2011, 52, 54–59. doi: 10.1134/S0022476611010070

[21] Zhang, Z.; Hu, L.; Wang, R.; Zhang, S.; Fu, L.; Li, M.; Xiao, Q. Advances in Monte Carlo Method for Simulating the Electrical Percolation Behavior of Conductive Polymer Composites with a Carbon-Based Filling. Polymers 2024, 16, 545. doi: 10.3390/polym16040545

[22] Gong, S., Zhu, Z. H., & Li, Z. Electron Tunnelling and Hopping Effects on the Temperature Coefficient of Resistance of Carbon Nanotube/Polymer Nanocomposites. Physical Chemistry Chemical Physics, 2017, 19(7), 5113–5120. doi: 10.1039/C6CP08115K

[23] Mora, A., Verma, P., and Kumar, S. "Electrical Conductivity of CNT/Polymer Composites: 3D Printing, Measurements and Modeling." Composites Part B: Engineering, vol. 183, 2020, article no. 107600. Elsevier, doi: 10.1016/j.compositesb.2019.107600

[24] Lin, T., Young, S.-L., Kung, C. Y., Chen, H., Kao, M.-C., Chang, M. C., & Chung-Jen, O. Variable-Range Hopping and Thermal Activation Conduction of Y-Doped ZnO Nanocrystalline Films. IEEE Transactions on Nanotechnology, 2014, 13, 425–430. doi: 10.1109/TNANO.2013.2280648

[25] Al-Shammari, H., Shukla, A., Asaad, A., & Kazi, S. N. Arrhenius Activation Energy and Thermal Radiation Effects on Oscillatory Heat-Mass Transfer of Darcy Forchheimer Nanofluid along Heat Generating Cone. Case Studies in Thermal Engineering, 2024, 57, Article 104294. doi: 10.1016/j.csite.2024.104294

[26] R. Bhatia, K. Kumari, R. Rani, A. Suri, U. Pahuja, and D. Singh, "A critical review of experimental results on low temperature charge transport in carbon nanotubes-based composites," Reviews in Physics, vol. 3, pp. 15–25, 2018, doi: 10.1016/j.revip.2017.12.001.

[27] R. M. Rudenko et al., "Effect of CNTs on PVDF/PANI/MWCNT nanocomposite," Diamond and Related Materials, vol. 143, p. 110924, 2024. doi: 10.1016/j.diamond.2024.110924

[28] Świniarski, M., Dużyńska, A., Gertych, A.P. et al. Determination of the electronic transport in type separated carbon nanotubes thin films doped with gold nanocrystals. Sci Rep 11, 16690 (2021). doi: 10.1038/s41598-021-96307-6

[29] Walter, D.; Bülau, A.; Zimmermann, A. Review on Excess Noise Measurements of Resistors. Sensors 2023, 23, 1107. doi: 10.3390/s23031107

[30] Palenskis, V.; Maknys, K. Nature of low-frequency noise in homogeneous semiconductors. Sci. Rep. 2016, 5, 18305. doi: 10.1038/srep18305

[31] L. M. Ward and P. E. Greenwood, "1/f noise," Scholarpedia, vol. 2, no. 12, p. 1537, 2007, revision no. 137265, doi: 10.4249/scholarpedia.1537.

[32] Lee, J.-K.; Pyo, J.; Kim, S. Low-Frequency Noise-Based Mechanism Analysis of Endurance Degradation in Al/αTiOx/Al Resistive Random-Access Memory Devices. Materials 2023, 16, 2317. doi: 10.3390/ma16062317

[33] Nah, J.; Perkins, F.K.; Lock, E.H.; Nath, A.; Boyd, A.; Myers-Ward, R.L.; Gaskill, D.K.; Osofsky, M.; Rao, M.V. Electrical and Low Frequency Noise Characterization of Graphene Chemical Sensor Devices Having Different Geometries. Sensors 2022, 22, 1183. doi: 10.3390/s22031183

[34] F. Bonani and G. Ghione, "Generation–recombination noise modelling in semiconductor devices through population or approximate equivalent current density fluctuations," Solid-State Electronics, vol. 43, no. 2, pp. 285–295, 1999, doi: 10.1016/S0038-1101(98)00253-6.

[35] White, David & Galleano, Roberto & Actis, A & Brixy, H & de Groot, Martin & Dubbeldam, J & Reesink, AL & Edler, F. & Sakurai, H & Shepard, R & Gallop, J.C. (2003). The status of Johnson noise thermometry. Metrologia. 33. 325. doi: 10.1088/0026-1394/33/4/6

[36] Gomila, Gabriel & Pennetta, C. & Reggiani, Lino & Sampietro, M & Ferrari, Giorgio & Bertuccio, Giuseppe. (2004). Shot Noise in Linear Macroscopic Resistors. Physical review letters. 92. 226601. doi: 10.1103/PhysRevLett.92.226601

[37] Tretjak, M., Palaimiene, E., Pralgauskaitė, S., Matukas, J., Banys, J., Macutkevič, J., Fierro, V., Schaefer, S., & Celzard, A. Noise and Electrical Characteristics of Composites Filled with Onion-Like Carbon Nanoparticles. Polymers, 2021, 13(7), 997. doi: 10.3390/polym13070997